Triclosan leads to dysregulation of the metabolic regulator FGF21 exacerbating high fat diet-induced nonalcoholic fatty liver disease

Mei-Fei Yueh[a], Feng He[b], Chen Chen[a], Catherine Vu[a], Anupriya Tripathi[c], Rob Knight[c], Michael Karin[b,1], Shujuan Chen[a], and Robert H. Tukey[a,1]

[a]Laboratory of Environmental Toxicology, Department of Pharmacology, University of California San Diego, La Jolla, CA 92093; [b]Laboratory of Gene Regulation and Signal Transduction, Department of Pharmacology, University of California San Diego, La Jolla, CA 92093; and [c]Department of Pediatrics, University of California San Diego, La Jolla, CA 92093

Contributed by Michael Karin, October 13, 2020 (sent for review August 13, 2020; reviewed by Christopher A. Bradfield and Bhagavatula Moorthy)

Triclosan (TCS), employed as an antiseptic and disinfectant, comes into direct contact with humans through a plethora of consumer products and its rising environmental release. We have demonstrated that TCS promotes liver tumorigenesis in mice, yet the biological and molecular mechanisms by which TCS exerts its toxicity, especially in early stages of liver disease, are largely unexplored. When mice were fed a high-fat diet (HFD), we found that fatty liver and dyslipidemia are prominent early signs of liver abnormality induced by TCS. The presumably protective HFD-induced hepatic expression of the metabolic regulator fibroblast growth factor 21 (FGF21) was blunted by TCS. TCS-altered *Fgf21* expression aligned with aberrant expression of genes encoding metabolic enzymes manifested as profound systemic metabolic changes that disturb homeostasis of amino acids, fatty acids, and glucose. Using a type 1 diabetic animal model, TCS potentiates and accelerates the development of steatohepatitis and fibrosis, accompanied by increased levels of hepatic lipid droplets and oxidative stress. Analysis of fecal samples revealed that HFD-fed mice exhibited a reduction in fecal species richness, and that TCS further diminished microbial diversity and shifted the bacterial community toward lower Bacteriodetes and higher Firmicutes, resembling changes in microbiota composition in nonalcoholic steatohepatitis (NASH) patients. Using reverse-genetic approaches, we demonstrate that, along with HFD, TCS induces hepatic steatosis and steatohepatitis jointly regulated by the transcription factor ATF4 and the nuclear receptor PPARα, which participate in the transcriptional regulation of the *Fgf21* gene. This study provides evidence linking nutritional imbalance and exposure to TCS with the progression of NASH.

toxicant-associated steatohepatitis | nonalcoholic steatohepatitis | high-fat diet | diabetes

Nonalcoholic fatty liver disease (NAFLD) has become the most common chronic liver condition and is the hepatic manifestation of metabolic syndrome, characterized by excessive lipid accumulation in hepatocytes. NAFLD is a precursor of a more severe form of metabolic liver inflammation, namely nonalcoholic steatohepatitis (NASH), and is associated with a twofold to threefold increased risk of developing type 2 diabetes (1). Along with hypernutrition as a prerequisite for steatosis and NASH, obesity, diabetes, and genetics play significant roles, although the precise mechanisms are unclear. Toxicant-associated steatohepatitis (TASH), caused by environmental and industrial chemicals, like NASH, is also characterized by hepatic steatosis accompanied by inflammatory infiltration and fibrosis in some cases (2). The rising prevalence of NASH and TASH associated with an epidemic of advanced liver disease mirrors increases in obesity and environmental toxicant exposure in modern life. Many preclinical models have been used to study the pathophysiology of fatty liver disease; among which, mice, especially MUP-uPA mice (3) fed a high-fat diet (HFD) exhibiting hepatic steatosis, have become a useful experimental animal model for research on NAFLD, NASH, and TASH (4).

The environmental contaminant triclosan (TCS) is a ubiquitous antimicrobial present in a myriad of consumer products as well as various environmental compartments. Ecotoxicology studies have showed that TCS is one of the most commonly encountered contaminants in solid and water compartments and has been detected in levels from nanograms to several micrograms per liter in sediments, sewage treatment plants, rivers, and lakes (5–7). In fact, TCS is listed among the seven most frequently detected compounds in streams across the United States, imposing a significant impact on aquatic ecosystems including waters that are used as sources of drinking water (8). Our previous study has shown that TCS can function as a liver tumor promoter stimulating liver tumorigenesis, due to, at least in part, the enhancement of liver oxidative stress and fibrosis (9, 10). Recent environmental toxicology studies suggest that exposure to TCS is associated with dysregulation of genes involved in lipid metabolism in toad tadpoles (11), and that it increased the level of lipids in the adult daphnids and induced lipid dislocation in newborn daphnids (12), providing a link of TCS to dyslipidemia.

Significance

While exploring triclosan-induced hepatoxicity, this study discovered that exposure to triclosan, in combination with a high-fat diet, causes nutritional imbalance, resulting in the pathogenesis of hepatic steatosis. The underlying mechanism through which triclosan imposes an impact on critical metabolic networks was delineated. The significance of this study lies in the fact that the ubiquitous presence of the environmental contaminant triclosan in conjunction with the prevalence of high consumption of dietary fat, which constitutes a good recipe for the development of fatty liver disease, are common factors encountered in everyday life. The finding that triclosan exacerbates high-fat diet-induced metabolic disorders by disrupting regulation of FGF21 expression provides a basis for a therapeutic approach in treating nonalcoholic fatty liver disease and steatohepatitis.

Author contributions: M.-F.Y., S.C., and R.H.T. designed research; M.-F.Y., F.H., C.C., C.V., A.T., and S.C. performed research; R.K. and M.K. contributed new reagents/analytic tools; M.-F.Y., M.K., S.C., and R.H.T. analyzed data; and M.-F.Y. and R.H.T. wrote the paper.

Reviewers: C.A.B., University of Wisconsin, Madison; and B.M., Texas Children's Hospital in Houston.

The authors declare no competing interest.

[1]To whom correspondence may be addressed. Email: mkarin@health.ucsd.edu or rtukey@health.ucsd.edu.

This article contains supporting information online at https://www.pnas.org/lookup/suppl/doi:10.1073/pnas.2017129117/-/DCSupplemental.

First published November 23, 2020.

The initiation of the study was the observation that TCS induces hepatic steatosis (fatty liver), an early sign of NAFLD/NASH or TASH, and that TCS blunts a HFD-induced expression of fibroblast growth factor 21 (FGF21) in the mouse liver. FGF21 is a liver-secreted cytokine critical for regulating hepatic metabolic processes including fat oxidation, gluconeogenesis, and metabolic gene expression (13). Ample experimental evidence indicated that FGF21 acts as a humoral signal that links nutrient sensing to metabolic and health outcomes. For example, chronic administration of FGF21 reverses hepatic steatosis and improves insulin sensitivity in obese mice (14). Interestingly, FGF21 is dysregulated in patients with NAFLD (15). Studying *Fgf21* regulation indicated that it is a target gene for the transcription-activating factor 4 (ATF4), a basic leucine zipper (bZIP) transcription factor that is preferentially translated in response to phosphorylation of eukaryotic translation initiation factor 2A (eIF2A), which reacts to a range of environmental, nutrient, and physiological stresses in addition to stresses afflicting the endoplasmic reticulum (ER), together referred to as the integrated stress response (ISR) (16, 17). Increased ATF4 protein synthesis, triggered by the ISR, enhances activation of its target genes, including *Fgf21*, tribbles homolog 3 (*Trib3*), and asparagine synthetase (*Asns*), which can collectively alleviate the ISR (18–20). Such results suggest that FGF21 induction by HFD activates a protective feedback response.

In parallel with regulation by ATF4, gene expression and circulating concentrations of FGF21 are also controlled by peroxisome proliferator-activated receptor α (PPARα), a nuclear receptor that serves as a key transcriptional regulator of numerous genes involved in lipid homeostasis. Mice lacking PPARα in the liver exhibited higher levels of free fatty acids in the blood and hepatic triglyceride accumulation (21). Synthetic PPARα agonists, such as fibrates, decrease circulating lipid levels and are commonly used to treat hyperlipidemia and other dyslipidemic states (22). Coincidentally, our experimental data showed that TCS is able to activate PPARα and induce its target gene *Cyp4a14* in the liver, most likely through an indirect mechanism (9).

In this study, we explored the impact of TCS together with HFD, demonstrating that TCS led to critical metabolic changes involving ATF4 and PPARα that impact transcriptional regulation of *Fgf21*, providing evidence for an underlying mechanism that links TCS to the development of NAFLD, NASH, and TASH. Under these conditions, TCS serves as a toxicant that promotes toxicant-associated fatty liver disease (TAFLD), which can progress to TASH (2, 23).

Materials and Methods

Animals and Diet. Male C57BL/6 mice (4 wk old) were fed with a chow diet or HFD (consisting of 59% fat, 15% protein, and 26% carbohydrates based on caloric content; Bio-Serv) containing 0.2% dimethyl sulfoxide (DMSO) as the control groups. As counterpart groups, the same age mice were fed with a diet (chow or HFD) containing 0.35 mM TCS dissolved in 0.2% DMSO ($n = 6$ to 8/group). After 4- to 4.5-mo TCS treatment, mice were killed, and their livers removed to be subject to analysis of gene expression and histological and immunochemical parameters. ATF4 liver conditional knockout $Atf4^{\Delta Hep}$ and control $Atf4^{F/F}$ mice were a generous gift from Dr. Christopher Adams (University of Iowa, Iowa City, IA). The *Pparα*-null ($Ppar\alpha^{-/-}$) mouse line was purchased from The Jackson Laboratory. NASH animal model: To induce mild islet inflammation and islet destruction, 2-d-old male neonates were subcutaneously administered a single injection of 200 μg of streptozotocin (STZ) and were fed with an HFD after being weaned at 4 wk (24). Mice were housed at the University of California San Diego (UCSD) Animal Care Facility; all animal use protocols, mouse handling, and experimental procedures were approved by the UCSD Animal Care and Use Committee; and these protocols were conducted in accordance with federal regulations.

Histological Examination, Oil Red O Staining, and Sirius Red Staining. To evaluate the severity of histological changes, livers were fixed in a 10% formalin phosphate buffer, and paraffin liver sections were prepared and stained with hematoxylin and eosin (H&E) at the Histology Core (UCSD). To visualize lipid droplets, cryosectioning of mouse liver tissue was prepared, and frozen sections were stained with Oil Red O (Sigma-Aldrich) as previously described (25). Hepatic collagen content was analyzed by Sirius Red staining (saturated picric acid containing 0.1% Sirius Red [Sigma-Aldrich]) of paraffin-embedded liver sections to assess the degree of fibrosis (9).

FGF21 Measurement by Enzyme-Linked Immunosorbent Assay, Serum Cholesterol Measurement, Alanine Aminotransferase Assay, and Determination of Serum Triglycerides. FGF21 levels in serum were measured by using the Mouse/Rat FGF21 Quantikine enzyme-linked immunosorbent assay (ELISA) kit (R&D System). Serum cholesterol levels were measured with the Cholesterol Fluorometric Assay kit (Cayman Chemical). Serum alanine aminotransferase (ALT)

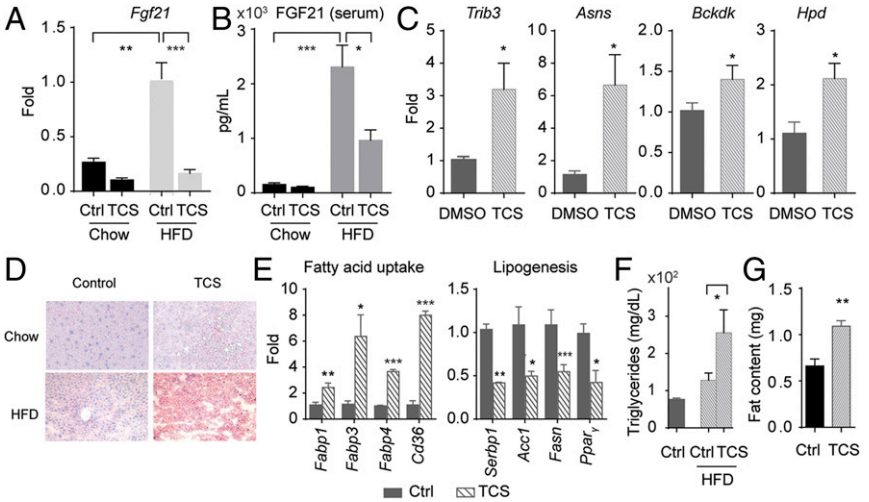

Fig. 1. TCS in combination with the high-fat diet (HFD) significantly blunted HFD-induced *Fgf21*, activated hepatic amino acid response (AAR), caused dyslipidemia, and altered triglycerides biosynthesis. Mice were fed with a chow diet, a chow diet containing TCS, an HFD, or an HFD containing TCS for 4 to 4.5 mo. (*A* and *B*) Hepatic FGF21 mRNA levels were measured by real-time PCR, and serum FGF21 levels were evaluated by the ELISA. (*C*) Mice were fed with an HFD containing either vehicle (DMSO) or TCS. Expression of hepatic genes involved in the AAR (*Trib3*, *Asns*) and genes associated with amino acid metabolism (*Bckdk*, *Hpd*) were evaluated by real-time PCR. (*D*) TCS increased lipid droplet accumulation in both a chow diet and HFD. (*E*) Under an HFD, TCS altered expression of genes associated with fatty acid uptake and lipogenesis. (*F*) TCS elevated serum triglyceride levels. (*G*) Under an HFD, TCS-treated mice had higher amounts of abdominal white adipose tissue.

activity was determined by the Infinity ALT kit (Thermo Fisher Scientific), and the Enzyme Linearity Test Set (Microgenics) was used for ALT standards. Serum triglyceride (TG) levels were assessed with Pointe Scientific Triglycerides Liquid Reagents (Thermo Fisher Scientific).

Glucose Tolerance Test. Mice were transferred to clean cages and were fasted for 6 h with access to drinking water. Small drops of blood were obtained from tail cuts and assessed for baseline glucose levels using a One-touch Ultra 2 glucometer (Lifescan; Johnson and Johnson). Blood was drawn and glucose levels were measured at the indicated time points after intraperitoneal injection of a 20% glucose solution (2 g/kg body weight).

Statistical Analysis. GraphPad Prism software (version 5) was used to analyze the data, which are presented as mean ± SD. Differences between two groups were compared using the two-tailed unpaired Student *t* test. Differences among multiple groups were compared using one-way analysis of variance. *P* values <0.05 were considered statistically significant, and statistically significant differences are indicated with $*P < 0.05$, $**P < 0.005$, and $***P < 0.0005$.

Descriptions for reverse transcription (RT) and real-time PCR, protein immunoblotting, isolation of primary hepatocytes, and 16S rRNA sequence processing are in *SI Appendix*.

Results

Effect of TCS on HFD-Induced FGF21 Levels and ISR Signaling. Recent findings have indicated a possible link between FGF21 and NAFLD (14, 15). In line with these findings, we found that mice fed an HFD for 18 wk exhibited significantly elevated FGF21 hepatic mRNA and circulating FGF21 levels compared with chow-fed mice (Fig. 1 *A* and *B*). As a critical target for the ISR, it is likely that FGF21 induction following HFD feeding represents an adaptive response that acts protectively to prevent hepatic lipid accumulation, counteract obesity, and improve insulin sensitivity (16, 17). Note that in combination with the HFD, TCS cotreatment greatly blunted the HFD-induced increase in FGF21, affecting both its mRNA and circulating levels (Fig. 1 *A* and *B*). Like *Fgf21*, activating transcription factor 3 (*Atf3*), *Aft5*, and C/EBP homologous protein (*Chop*) are target genes of ISR, and TCS also exerted similar effects by counteracting the induction of these genes by an HFD (*SI Appendix*, Fig. S1). These data indicate that chronic exposure of TCS disrupts HFD-mediated FGF21 regulation and ISR signaling.

Metabolic Effects of TCS. FGF21 signaling has emerged as an important regulator of several key metabolic processes (20, 26). The dysregulation of *Fgf21* expression by TCS during an HFD prompted us to explore the impact of TCS cotreatment on genes associated with energy metabolism, particularly homeostasis of amino acids, fatty acids, and glucose.

Amino acid metabolism. Activation of ISR has been linked to various forms of cellular stress, including amino acid imbalance (27). It is known that ISR can be potentially activated upon conditions deprived of one or more essential amino acids, which in turn enhances essential amino acid biosynthesis (28), a response known as the amino acid response (AAR), which is observed during protein restriction. We found that under HFD, TCS cotreatment mimics amino acid deficiency and activates the AAR as TCS induced expression of the AAR markers *Asns* and *Trib3* (Fig. 1*C*). Expression of hepatic genes associated with amino acid metabolism, including branched chain ketoacid dehydrogenase kinase (*Bckdk*) and 4-hydroxyphenylpyruvic acid dioxygenase (*Hpd*), was altered by TCS. These results imply that TCS exposure aggravates protein deficiency during the HFD.

Hepatic lipid droplet accumulation. The presence of lipid droplets in the liver is considered an early sign of liver pathogenesis (29). Histological studies using Oil Red O staining indicated that TCS promoted accumulation of lipid droplets, which appeared as early as 10 wk following TCS treatment in mice fed either normal chow or HFD (Fig. 1*D*).

Alteration of genes associated with lipid metabolism. Examination of the hepatic gene expression profile indicated that mice fed HFD together with TCS exhibited dysregulation of lipid metabolic genes. Increased expression of genes associated with fatty acid uptake, including fatty acid binding protein 1 (*Fabp1*), *Fabp3*, *Fabp4*, and fatty acid translocase *Cd36*, was observed. A recent study has reported that HFD suppresses de novo lipogenesis (30), and our results showed that TCS cotreatment exacerbated the reduction in lipogenesis. Compared with the HFD-only group, genes associated with lipogenesis were down-regulated by TCS, including sterol regulatory element binding protein 1C (*Serbp1c*), acetyl-coA carboxylase 1 (*Acc1*), fatty-acid synthase (*Fasn*), and peroxisome proliferator-activated receptor γ (*Pparγ*) (Fig. 1*E*). With increased uptake of fatty acids and lower lipogenesis, the TCS group mice appeared to have much greater rates of TG synthesis, compared with mice given HFD only (Fig. 1*F*). The significant impact of TCS on hepatic lipid metabolism and systemic TG accompanied by lower FGF21 is generally consistent with previous studies demonstrating that FGF21 signaling impacts a variety of metabolic processes including lipogenesis and TG synthesis (14, 31).

Alteration of bile acid metabolism and cholesterol. HFD in combination with TCS suppressed expression of *Lxrα* and *Cyp7b1* (*SI Appendix*, Fig. S2*A*), both of which have been indicated in maintaining cholesterol homeostasis (32–34). Furthermore, we found that TCS has a cholesterol-lowering effect when mice were fed either normal chow or HFD (*SI Appendix*, Fig. S2*B*).

Alteration in fat content in adipose tissue. Adipose tissue is a target organ of FGF21 action. Despite having a slightly lower food intake and lower body weight, TCS-treated mice exhibited more than a 50% increase in fat content of abdominal adipose tissue, indicating that TCS may promote fat uptake and allocate lipids to adipose tissue (Fig. 1*G*). Overall, these results indicate that fatty acid uptake and lipogenesis as well as TG and cholesterol levels were impacted by TCS exposure.

Insulin tolerance. The fact that FGF21 plays a role in attenuating hyperglycemia and that insulin sensitivity is one of the major risk factors for NAFLD (35), led us to postulate that TCS may influence glucose tolerance. Although it was not statistically significant, lower FGF21 was correlated with higher blood glucose (hyperglycemia) in the TCS group than those in the normal chow or HFD-alone groups (*SI Appendix*, Fig. S3*A*). Increasing evidence suggests that stearoyl-CoA desaturase (SCD), the rate-limiting enzyme of monounsaturated fatty acid biosynthesis, is an important factor in the pathogenesis of lipid-induced insulin resistance. The results of real-time PCR showed that together with HFD TCS induced both SCD1 and SCD2 mRNAs (*SI Appendix*, Fig. S3*B*). These results are in line with the previous findings that mice with a targeted disruption of *Scd1* have improved glucose tolerance compared to wild-type mice (36).

TCS Facilitates the Development of NASH. By administering a single dose of STZ to 2-d-old neonatal mice to damage insulin-secreting beta cells in the pancreas (24) and placing these animals on HFD, we established a model in which mice robustly developed steatosis at 7 to 8 wk of age followed by steatohepatitis at 10 to 12 wk. When STZ-injected mice underwent a 10-wk TCS treatment, they exhibited elevated ALT, increased accumulation of lipid droplets, and worsening of histological manifestations (Fig. 2 *A*–*C*), indicating that TCS potentiates liver pathogenesis and accelerates the development of NASH. To examine the underlying pathological changes at the gene expression level, we used real-time PCR analysis, which indicated that TCS-treated mice exhibited elevated levels of oxidative stress, hepatic fibrosis, and inflammatory responses. This was evidenced by higher expression of oxidative stress responsive genes (*Ho-1*, *Gsta1*, and *Gsta2*), fibrogenic genes (*Collagen 1a1* and *Timp1*), and proinflammatory cytokines (*Tnfα* and *Il-8*) (Fig. 2*D*). The

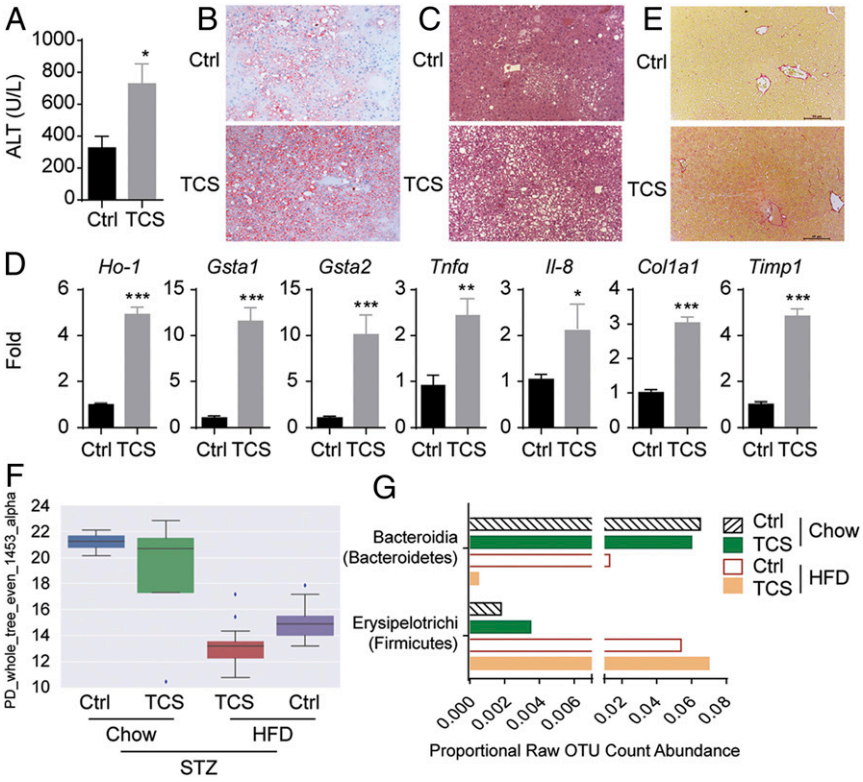

Fig. 2. TCS impaired liver function, exasperated steatohepatitis, and impacted microbiota composition in the study using the type I diabetic animal model. Male neonatal mice were administered with streptozotocin (STZ) followed by high-fat diet (HFD) feeding, containing either vehicle (ctrl) or TCS, for ~10 wk after they were weaned. (*A*) Serum ALT levels. (*B*) Hepatic lipid droplets detected by Oil Red O staining. (*C*) Histological analysis with H&E staining. (*D*) Expression of genes, including (*i*) *Ho-1*, *Gsta1*, *Gsta2*, (*ii*) *Tnfα*, *Il-8*, and (*iii*) *Collagen 1a1*, *Timp1*, was quantitated using real-time PCR. (*E*) Representative Sirius red staining of liver sections shows collagen deposition, indicating fibrosis progression in the TCS-treated mice compared with control mice. (*F* and *G*) STZ-injected male mice (14 wk old) were subjected to a chow diet containing vehicle (Ctrl) or TCS, or a high-fat diet containing vehicle (HFD) or TCS (HFD + TCS). (*F*) Microbial diversity analysis revealed that an HFD led to decreases in bacterial diversity, and TCS further significantly reduced the species diversity in the gut microbial community. (*G*) The HFD group had decreased fecal Bacteroidetes and increased Firmicutes, and the changes were synergistically enlarged when mice were fed an HFD containing TCS.

worsening of hepatic fibrosis in TCS-treated mice was also illustrated by collagen deposition detected by Sirius Red staining (Fig. 2*E*). These results demonstrate that TCS promotes inflammatory responses and accelerates development of steatohepatitis in the type I diabetic animal model.

Microbial Basis for TCS-Induced NAFLD. Depending on its concentration, TCS is either bactericidal or bacteriostatic, targeting the final step of bacterial fatty acid synthesis (37). Accordingly, we postulated that TCS may alter the gut microbial community, further impacting TASH development. To assess how TCS influences microbiota composition, we collected fecal samples of 14-wk-old mice in STZ-injected mice fed either HFD alone or HFD containing TCS, followed by DNA isolation, 16S ribosomal RNA sequencing, and microbial community diversity analysis. The results showed that HFD led to decreased bacterial diversity, and TCS further reduced the species diversity of gut microbial communities (Fig. 2*F*). These results are consistent with those of a clinical study that included healthy controls, obese subjects without known liver diseases, and patients with biopsy-proven NASH: Fecal species richness was diminished in obese subjects and NASH patients compared to controls (38). Following taxonomic classifications and gene annotations, we further uncovered that both Bacteroidetes and Firmicutes are significantly altered by the HFD as the HFD group had decreased fecal Bacteroidetes and increased Firmicutes, and the changes are synergistically enlarged when mice were treated with TCS along with an HFD (Fig. 2*G*). These results are in line with previous findings in animals and resemble what was observed clinically, that NASH patients had decreased fecal Bacteroidetes and increased Firmicutes (39). These data suggest a microbial basis for the etiology of TCS-mediated TASH.

ATF4 Controls *Fgf21* Expression in Response to ISR Triggered by TCS. Our findings indicate the involvement of FGF21 in TCS-induced nutritional stress and liver pathogenesis. We further explored the underlying mechanism that dictates TCS-mediated FGF21 dysregulation and found that hyperinduction of ATF4 protein expression occurred when mice ($n = 4$) were cotreated with TCS together with HFD. The induction of ATF4 at the translational level was accompanied by an elevated phosphorylation of eIF2A (Fig. 3*A*). It is well established that the phosphorylation of eIF2A induces ATF4 translational expression in response to a range of environmental and physiological stresses, and this regulatory scheme has been referred to as the ISR (17). As a mediator of the nutrient-sensing response pathway, ATF4 has a direct impact on glucose, amino acid, and fatty acid metabolism, via target genes, including *Fgf21*, *Trib3*, and *Asns* (18). In vitro experiments with primary hepatocytes isolated from either control ($Atf4^{F/F}$) or liver-specific ATF4 knockout ($Atf4^{\Delta Hep}$) mice revealed that, following 72-h TCS treatment, lipid droplet accumulation only appeared in the control mice but not in ATF4-deficient hepatocytes (*SI Appendix*, Fig. S4). Next, control and $Atf4^{\Delta Hep}$ mice underwent a 4-mo HFD with or without TCS

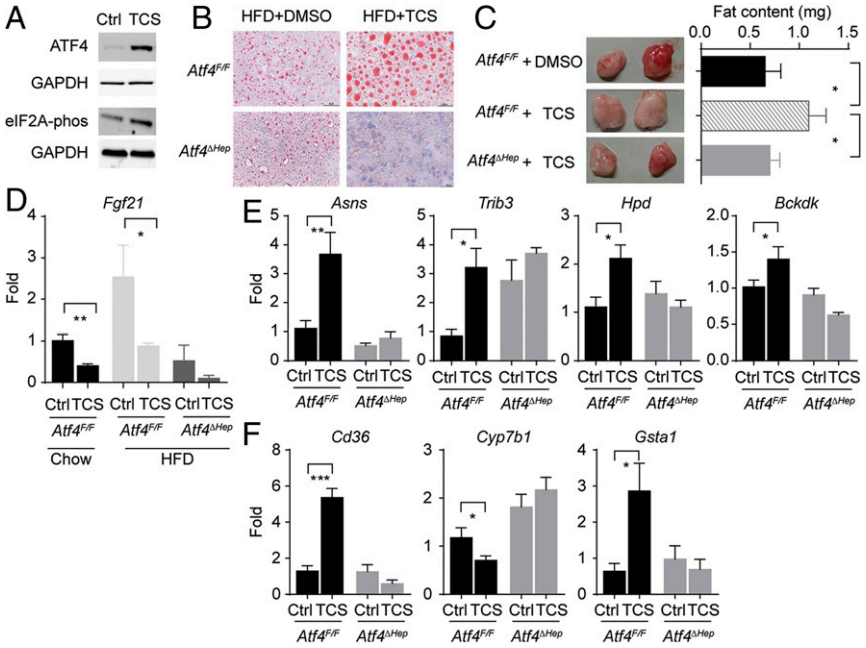

Fig. 3. ATF4 is highly induced in TCS-treated mice and is required for TCS-induced dyslipidemia. (*A*). Mice ($n = 4$) were subjected to a high-fat diet (HFD) containing either vehicle (Ctrl) or TCS. Hyperactivation of ATF4 at the protein level (*Left*) and phosphorylation of eukaryotic translation initiation factor 2A (eIF2A) (*Right*) by TCS detected by Western blotting. (*B–E*) $Atf4^{F/F}$and $Atf4^{\Delta Hep}$ mice were fed an HFD containing either vehicle or TCS. (*B*) Oil Red O staining shows that lipid droplets were significantly reduced in the liver slide obtained from $Atf4^{\Delta Hep}$ mice. (*C*) The abdominal fat content in the control $Atf4^{F/F}$ or $Atf4^{\Delta Hep}$ mice, with two representatives of each group shown in the pictures. (*D*) Fgf21 gene expression was determined by real-time PCR. (*E* and *F*) Real-time PCR analysis of genes impacted by TCS.

treatment; Oil Red O staining of mouse liver tissue showed that the size of lipid droplets significantly reduced in the $Atf4^{\Delta Hep}$ mice (Fig. 3*B*). Moreover, the increase in abdominal fat content induced by TCS was diminished in the $Atf4^{\Delta Hep}$ mice (Fig. 3*C*). These results indicate that TCS-induced lipid uptake in hepatocytes and adipose tissue is ATF4 dependent.

As we further examined the gene expression profile in $Atf4^{\Delta Hep}$ mice, real-time PCR results showed that TCS-induced dysregulation of *Fgf21* was blocked in the $Atf4^{\Delta Hep}$ mice (Fig. 3*D*), confirming the role of ATF4 in controlling *Fgf21* gene expression in response to ISR triggered by TCS. Similarly, the induction of genes associated with amino acid metabolism by TCS, including *Asna*, *Trib3*, *Hpd*, and *Bckdk*, was absent in the $Atf4^{\Delta Hep}$ mice (Fig. 3*E*), indicating that AAR prompted by TCS requires ATF4. Furthermore, regulation of *Cd36* and *Cyp7b1* and induction of the oxidative stress gene *Gsta1* by TCS also appear to be ATF4 dependent (Fig. 3*F*). These data indicate that liver-derived ATF4 has a direct impact on *Fgf21* transcriptional regulation by TCS and is attributed to TCS-induced metabolic effects, particularly on lipid and amino acid metabolism.

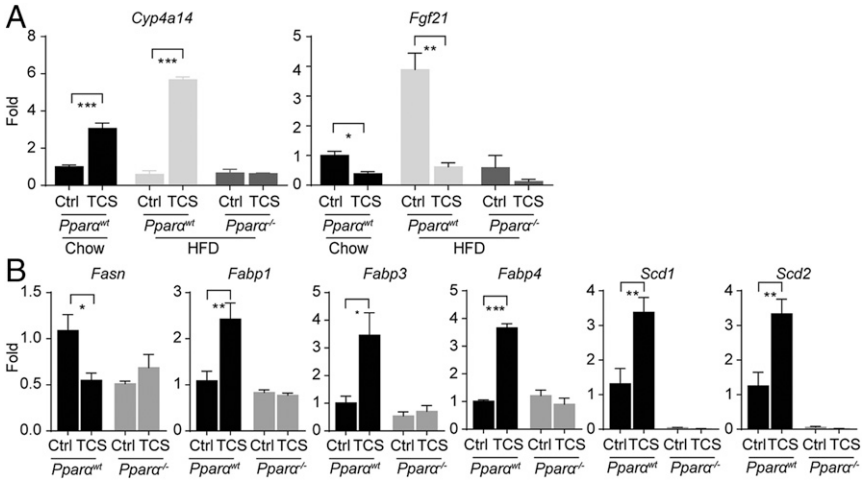

Fig. 4. Induction of *Cyp4a14* by TCS is PPARα dependent. (*A*) Mice ($Ppar\alpha^{wt}$ or $Ppar\alpha^{-/-}$) were subjected to a chow diet containing vehicle (Ctrl) or TCS, or a high-fat diet (HFD) containing vehicle (Ctrl) or TCS. TCS-induced *Cyp4a14* expression was diminished in *Ppaα* knockout mice (*Left*). *Ffg21* expression regulated by an HFD and HFD/TCS is PPARα dependent (*Right*). (*B*) Mice ($Ppar\alpha^{wt}$ or $Ppar\alpha^{-/-}$) were subjected to a HFD-containing vehicle (Ctrl) or TCS. PPARα-dependent gene regulation was detected by real-time PCR.

Involvement of PPARα in TCS-Altered Lipid Metabolism. Hepatic CYP4A14 is a homolog of human CYP4A hydroxylase that catalyzes omega-hydroxylation of medium-chain fatty acids and arachidonic acid in mice. Induction of *Cyp4a14* through PPARα has been linked to the pathogenesis of lipid dysregulation and NAFLD (40–42). Notably, hepatic *Cyp4a14* was pronouncedly induced when mice were exposed to TCS, especially in combination with HFD (Fig. 4*A*). To further delineate the role of PPARα in TCS-induced dyslipidemia, we fed control and *Pparα*-deficient ($Ppar\alpha^{-/-}$) mice HFD with or without TCS. The gene expression profile showed that PPARα not only plays a critical role in TCS-induced *Cyp4a14*; equally importantly, *PPARα* is required for the transcriptional regulation of *Fgf21* by both HFD and TCS (Fig. 4*A*). Compared with HFD-fed control mice in which *Fasn* was down-regulated by TCS, this effect was abolished in $Ppar\alpha^{-/-}$ mice (Fig. 4*B*). Similarly, expression of genes involved in hepatic lipogenesis, including *Fabp1*, *Fabp3*, and *Fabp4*, was induced by TCS in control mice and became resistant to TCS in *Pparα*-deficient mice (Fig. 4*B*). We further demonstrated that PPARα is involved in TCS-induced SCD1 and SCD2 mRNA expression, supporting the notion that TCS promotes insulin resistance, potentially through PPARα-regulated *Scd* gene expression (Fig. 4*B*). These results suggest that in addition to the ATF4-mediated ISR signaling pathway, PPARα-dependent regulation influencing *Cyp4a14* expression and lipid metabolism also contributes to the development and progression of TAFLD.

Discussion

Environmental exposures to a host of chemicals have been linked to the development of TAFLD, a pathological condition covering a spectrum of liver injuries that resembles NAFLD, which together affect staggering numbers of individuals globally. The premise of this study was the discovery of TCS, similar to an HFD, being an inducer for fatty liver disease and that combining TCS exposure with HFD would accelerate progression to NASH. This study illustrates critical metabolic networks, entailing ATF4 and PPARα signaling, that are susceptible to TCS in conjunction with HFD and contribute to the pathogenesis of steatosis and steatohepatitis.

FGF21 has emerged as a novel therapeutic agent for the treatment of metabolic syndrome; studies have indicated that FGF21 exerts beneficial effects on glucose, lipid, and energy metabolism in mice and humans. Induction of FGF21 following HFD in mice is associated with the adaptive response to nutrition imbalance as chronic administration of FGF21 reverses hepatic steatosis and improves insulin sensitivity in obese mice (14). In clinical studies, FGF21 analogs have also been demonstrated to elicit similar effects that improve dyslipidemia and insulin insensitivity in obese patients with type 2 diabetes (43, 44). Interestingly, FGF21 mRNA is increased sixfold in patients with NAFLD, whereas patients with NASH had lower FGF21 compared to NAFLD. Lower hepatic FGF21 expression in NASH compared to NAFLD may reflect more advanced hepatic injury (15); this phenomenon also occurred in TCS-treated mice as we have observed lower FGF21 in these mice compared with control mice treated with an HFD alone. When we explored the molecular mechanism underlying TCS-induced NASH, our results showed that TCS-treated mice with dysregulated FGF21 exhibited a distinct metabolic signature associated with energy imbalance. FGF21 dysregulation by TCS was associated with aberrant expression of genes encoding metabolic enzymes, manifesting as imbalance of amino acid metabolism, dyslipidemia, and insulin resistance.

eIF2A-dependent activation of ATF4 is an important mediator of the unfolded protein response and acts as a switch to up-regulate the transcription of a specific set of stress response genes when overall translation is depressed (16, 17). ATF4 plays a key role in regulating energy homeostasis, partially through controlling expression of the *Fgf21* gene to allow adaptation to metabolic stress (19, 20). Studies have found that ATF4-deficient mice resist diet-induced obesity, hyperlipidemia, and hepatosteatosis (45). In line with the previous finding that ATF4 has direct functions in amino acid and fatty acid metabolism, TCS-induced hepatic ATF4 translation was accompanied by hepatic lipid droplet accumulation, changes in expression of genes associated with lipid and amino acid metabolism, increased serum TG, and higher fat content in adipose tissue, together eliciting the ISR. Translational induction of ATF4 along with abnormal metabolic profiles following TCS treatment is consistent with the notion that preferential translation of ATF4 functions as a hallmark of ISR (16). In contrast, primary hepatocytes of the liver-specific *Atf4* knockout mouse failed to exhibit TCS-induced lipid droplet accumulation, suggesting that ATF4 is required for the formation of hepatic lipid droplets during the early stage of fatty liver disease. Using liver-specific knockout mice, we further demonstrated that TCS-mediated alterations of genes associated with the metabolism of amino acids (i.e., *Asns*, *Trib3*, *Hpd*, and *Bckdk*), fatty acids, and bile acids (i.e., *Cd36* and *Cyp7b1*) as well as oxidative stress (i.e., *Gsta1*) were ATF4 dependent. Notedly, in the absence of hepatic ATF4, *Fgf21* gene expression levels were drastically decreased following HFD compared with those of control mice, implying that *Fgf21* induction by the HFD is severely impaired in $Atf4^{\Delta Hep}$ mice; under such a condition in which *Fgf21* expression is severely suppressed, adding TCS to the HFD did not affect *Fgf21* expression.

In addition to its key role in regulating β-oxidation, PPARα has been shown to positively regulate the expression of genes controlling fatty acid uptake and biosynthesis, including *Cyp4a14* and *Fgf21* (40, 42, 46). Although TCS did not directly activate PPARα based on the results of the luciferase reporter assay (9), the in vivo study described here showed that *Cyp4a14* was abundantly induced in the liver by TCS, especially in HFD-fed mice. By contrast, induction of *Cyp4a14* was completely abolished in *Pparα* knockout mice, indicating that TCS may activate PPARα through an indirect mechanism. Regardless of *Fgf21* regulation by TCS, TCS-mediated *Cyp4a14* gene induction through PPARα could contribute to changes in lipid metabolism based on the fact that 1) the hepatic *CYP4A* expression was up-regulated in the livers of patients and three murine models of NAFLD; 2) overexpression of *Cyp4a14* in the livers of C57BL/6 mice resulted in a fatty liver phenotype; and 3) inhibition of CYP4A attenuated, whereas induction of CYP4A promoted, hepatic ER stress, and apoptosis in diabetic mice (40–42). It is possible that elevated liver fat stimulated by TCS—presumably through dysregulation of the ATF4/FGF21 axis—acts as a natural endogenous agonist to activate PPARα, which in turn stimulates induction of *Cyp4a14*, as evidenced by lower FGF21 and higher *Cyp4a14* expression observed in TCS-treated mice under the HFD, and both regulations are completely abolished in PPARα-deficient mice. It will be of importance to delineate the individual role of FGF21 and CYP4A14 in TCS-induced dyslipidemia. Nevertheless, this study connects TCS-induced PPARα activation with the regulation of genes involving fatty acid metabolism and insulin resistance, potentially linking CYP4A14 and/or FGF21 to downstream genes associated with metabolic disorder. These data support the concept that the activation of the PPARα-dependent peroxisomal β-oxidation pathway by TCS provides an alternative mechanism underlying the development of hepatic steatosis.

Similar to regulation by ATF4, induction of FGF21 by HFD was severely diminished in *Pparα* knockout mice, suggesting that the metabolic transition initiated by the HFD involves a signal transduction pathway controlled by both ATF4 and PPARα. When the second phase of the metabolic transition caused by TCS exposure occurs, in contrast to the fluctuation of *Fgf21*

levels observed in HFD-fed control mice, no significant variation of *Fgf21* levels was observed in either $Atf4^{\Delta Hep}$- or *Pparα*-deficient mice when mice were exposed to HFD plus TCS. These results may imply that TCS-mediated FGF21 dysregulation may not take place in *Atf4*- or *Pparα*-knockout mice and that hepatic dyslipidemia would have improved in the absence of either of these two proteins. However, the overall systemic impact of TCS toxicity through respective individual signaling pathways needs further investigation.

In the context of HFD-induced NAFLD, TCS-mediated signaling disrupts conventional FGF21 regulation controlled by ATF4 and FGF21 in response to high fat consumption. TCS acts as an FGF21 antagonist, which is opposite to other known metabolic factors—including protein restriction, energy restriction, and ketogenic diet—that positively affect FGF21. It is of particular interest to delineate FGF21 downstream signaling, ultimately impacting TCS-mediated alterations in macronutrient metabolism. It is also important to find out whether the gene expression and circulating concentrations of FGF21 are regulated divergently by ATF4 and PPARα, or cooperatively controlled by an overlapping downstream signaling pathway. Furthermore, some of the results derived from this study deserve further investigation: 1) Although the role of FGF21 in biosynthesis and/or metabolism of TG, cholesterol, and bile acids is well established, the direct link of its involvement in TCS-mediated metabolic changes is necessary to be confirmed by experimental models such as FGF21 deficiency mice. 2) Given that TCS has a cholesterol-lowering effect when mice are treated with either a chow diet or HFD (*SI Appendix*, Fig. S2*A*), it is worth exploring the regulatory pathway controlling TCS's cholesterol-lowering ability. 3) TCS promotes fat intake in the liver and abdominal adipose tissue. Increased intraabdominal/visceral fat, belonging to white adipose tissue, is associated with a high risk of metabolic disease (47). While the distribution of white adipose tissue greatly affects metabolic risk, it would be important to also evaluate the effect of TCS on the composition of brown adipose tissue, which is crucial for thermogenesis and energy balance, in the interscapular area.

Using a type 1 diabetic animal model, we further explored how TCS affects the pathophysiology of steatohepatitis. When STZ-induced diabetic mice were fed HFD, TCS exposure accelerated the development of NASH as evidenced by increased collagen deposition, increased proinflammatory responses, and elevated oxidative stress. These data support the notion that, like HFD, TCS can be one of the major contributors to the pathogenesis of steatohepatitis. Furthermore, we provide evidence that TCS along with HFD induced dysbiosis of gut microbiota and diminished the bacterial diversity, with a higher Firmicutes/Bacteroidetes ratio. Intestinal microbiota imbalance has been documented in obese individuals or those with NASH and metabolic syndrome. A decrease of total bacterial diversity/richness as well as a reduced proportion of Bacteroidetes and increased Firmicutes have been indicated as a main feature of metabolic syndrome-related intestinal dysbiosis in humans (39, 48). In nutritional models of obesity in mice using the HFD, an increased Firmicutes/Bacteroidetes ratio is also a common outcome (49), and our data indicate that TCS exacerbates a state of microbial imbalance. Considering elevated inflammatory responses induced by TCS, one potential underlying mechanism linking TCS to the pathway of the gut–liver axis is that TCS may play a role in compromising the intestinal barrier function, leading to the increase of gut-derived toxins in systemic circulation constituting metabolic endotoxemia, which in turn contributes to the manifestation of a chronic inflammation state as we observed in TCS-treated mice. This hypothesis would be worth further exploring.

In this study, mice received ∼15 mg/kg TCS daily, based on a diet of 3 g of daily chow at the concentration of 100 ppm. When blood samples were analyzed by global metabolomic analysis, the results revealed that the TCS concentrations in mice were comparable to what have been identified in human blood samples (50). This study provides a mechanistic basis for how TCS affects metabolic networks in mice, and how to translate our findings to human health still needs further exploration.

In summary, this study illustrates critical metabolic networks—entailing ATF4- and PPARα-directed regulatory schemes—that are susceptible to the combination of TCS and an HFD, which ultimately impact FGF21 levels. Through these metabolic pathways, TCS creates a pathological condition manifesting as profound metabolic changes affecting all aspects of energy balance, including amino acid, lipid, and glucose metabolism, contributing to the pathogenesis of NAFLD.

Data Availability. All study data are included in the article and *SI Appendix*.

ACKNOWLEDGMENTS. This work was supported by National Institute of Environmental Health Sciences Grant ES010337 (R.H.T. and M.K.) and NIH Grants R21-ES023906 (M.-F.Y.), R21-AI135677 (S.C.), GM126074 (R.H.T.), CA211794 (M.K.), CA198103 (M.K. and R. Kauffman), and DK120714 (M.K.). M.K. is an American Cancer Society Research Professor and holder of the Ben and Wanda Hildyard Chair for Mitochondrial and Metabolic Diseases. F.H. was funded in part by a fellowship from Eli Lilly. 16S sequencing was supported in part by a seed grant from the Center for Microbiome Innovation.

1. E. Fabbrini, S. Sullivan, S. Klein, Obesity and nonalcoholic fatty liver disease: Biochemical, metabolic, and clinical implications. *Hepatology* **51**, 679–689 (2010).
2. B. Wahlang *et al.*, Toxicant-associated steatohepatitis. *Toxicol. Pathol.* **41**, 343–360 (2013).
3. M. A. Febbraio *et al.*, Preclinical models for studying NASH-driven HCC: How useful are they? *Cell Metab.* **29**, 18–26 (2019).
4. K. Stephenson *et al.*, Updates on dietary models of nonalcoholic fatty liver disease: Current studies and insights. *Gene Expr.* **18**, 5–17 (2018).
5. D. C. McAvoy, B. Schatowitz, M. Jacob, A. Hauk, W. S. Eckhoff, Measurement of triclosan in wastewater treatment systems. *Environ. Toxicol. Chem.* **21**, 1323–1329 (2002).
6. G. Bedoux, B. Roig, O. Thomas, V. Dupont, B. Le Bot, Occurrence and toxicity of antimicrobial triclosan and by-products in the environment. *Environ. Sci. Pollut. Res. Int.* **19**, 1044–1065 (2012).
7. M. J. Gómez, M. J. Martínez Bueno, S. Lacorte, A. R. Fernández-Alba, A. Agüera, Pilot survey monitoring pharmaceuticals and related compounds in a sewage treatment plant located on the Mediterranean coast. *Chemosphere* **66**, 993–1002 (2007).
8. D. R. Orvos *et al.*, Aquatic toxicity of triclosan. *Environ. Toxicol. Chem.* **21**, 1338–1349 (2002).
9. M. F. Yueh *et al.*, The commonly used antimicrobial additive triclosan is a liver tumor promoter. *Proc. Natl. Acad. Sci. U.S.A.* **111**, 17200–17205 (2014).
10. M. F. Yueh, R. H. Tukey, Triclosan: A widespread environmental toxicant with many biological effects. *Annu. Rev. Pharmacol. Toxicol.* **56**, 251–272 (2016).
11. L. Chai, A. Chen, P. Luo, H. Zhao, H. Wang, Histopathological changes and lipid metabolism in the liver of *Bufo gargarizans* tadpoles exposed to triclosan. *Chemosphere* **182**, 255–266 (2017).
12. N. Sengupta, D. C. Reardon, P. D. Gerard, W. S. Baldwin, Exchange of polar lipids from adults to neonates in *Daphnia magna*: Perturbations in sphingomyelin allocation by dietary lipids and environmental toxicants. *PLoS One* **12**, e0178131 (2017).
13. F. M. Fisher, E. Maratos-Flier, Understanding the physiology of FGF21. *Annu. Rev. Physiol.* **78**, 223–241 (2016).
14. J. Xu *et al.*, Fibroblast growth factor 21 reverses hepatic steatosis, increases energy expenditure, and improves insulin sensitivity in diet-induced obese mice. *Diabetes* **58**, 250–259 (2009).
15. J. Dushay *et al.*, Increased fibroblast growth factor 21 in obesity and nonalcoholic fatty liver disease. *Gastroenterology* **139**, 456–463 (2010).
16. H. P. Harding *et al.*, An integrated stress response regulates amino acid metabolism and resistance to oxidative stress. *Mol. Cell* **11**, 619–633 (2003).
17. T. D. Baird, R. C. Wek, Eukaryotic initiation factor 2 phosphorylation and translational control in metabolism. *Adv. Nutr.* **3**, 307–321 (2012).
18. F. Siu, P. J. Bain, R. LeBlanc-Chaffin, H. Chen, M. S. Kilberg, ATF4 is a mediator of the nutrient-sensing response pathway that activates the human asparagine synthetase gene. *J. Biol. Chem.* **277**, 24120–24127 (2002).
19. C. D. Morrison, T. Laeger, Protein-dependent regulation of feeding and metabolism. *Trends Endocrinol. Metab.* **26**, 256–262 (2015).
20. A. L. De Sousa-Coelho *et al.*, FGF21 mediates the lipid metabolism response to amino acid starvation. *J. Lipid Res.* **54**, 1786–1797 (2013).

21. A. Montagner *et al*., Liver PPARα is crucial for whole-body fatty acid homeostasis and is protective against NAFLD. *Gut* **65**, 1202–1214 (2016).
22. K. Schoonjans, B. Staels, J. Auwerx, The peroxisome proliferator activated receptors (PPARS) and their effects on lipid metabolism and adipocyte differentiation. *Biochim. Biophys. Acta* **1302**, 93–109 (1996).
23. M. Cave *et al*., Toxicant-associated steatohepatitis in vinyl chloride workers. *Hepatology* **51**, 474–481 (2010).
24. M. Fujii *et al*., A murine model for non-alcoholic steatohepatitis showing evidence of association between diabetes and hepatocellular carcinoma. *Med. Mol. Morphol.* **46**, 141–152 (2013).
25. T. S. Jung *et al*., α-Lipoic acid prevents non-alcoholic fatty liver disease in OLETF rats. *Liver Int.* **32**, 1565–1573 (2012).
26. M. L. Reitman, FGF21: A missing link in the biology of fasting. *Cell Metab.* **5**, 405–407 (2007).
27. C. Jousse *et al*., TRB3 inhibits the transcriptional activation of stress-regulated genes by a negative feedback on the ATF4 pathway. *J. Biol. Chem.* **282**, 15851–15861 (2007).
28. F. Guo, D. R. Cavener, The GCN2 eIF2alpha kinase regulates fatty-acid homeostasis in the liver during deprivation of an essential amino acid. *Cell Metab.* **5**, 103–114 (2007).
29. J. Cao *et al*., Saturated fatty acid induction of endoplasmic reticulum stress and apoptosis in human liver cells via the PERK/ATF4/CHOP signaling pathway. *Mol. Cell. Biochem.* **364**, 115–129 (2012).
30. J. A. Duarte *et al*., A high-fat diet suppresses de novo lipogenesis and desaturation but not elongation and triglyceride synthesis in mice. *J. Lipid Res.* **55**, 2541–2553 (2014).
31. J. Huang *et al*., Development of a novel long-acting antidiabetic FGF21 mimetic by targeted conjugation to a scaffold antibody. *J. Pharmacol. Exp. Ther.* **346**, 270–280 (2013).
32. A. R. Stiles, J. G. McDonald, D. R. Bauman, D. W. Russell, CYP7B1: One cytochrome P450, two human genetic diseases, and multiple physiological functions. *J. Biol. Chem.* **284**, 28485–28489 (2009).
33. H. Uppal *et al*., Activation of LXRs prevents bile acid toxicity and cholestasis in female mice. *Hepatology* **45**, 422–432 (2007).
34. T. Wada *et al*., Identification of oxysterol 7alpha-hydroxylase (Cyp7b1) as a novel retinoid-related orphan receptor alpha (RORalpha) (NR1F1) target gene and a functional cross-talk between RORalpha and liver X receptor (NR1H3). *Mol. Pharmacol.* **73**, 891–899 (2008).
35. B. Emanuelli *et al*., Interplay between FGF21 and insulin action in the liver regulates metabolism. *J. Clin. Invest.* **124**, 515–527 (2014).
36. P. Dobrzyn, M. Jazurek, A. Dobrzyn, Stearoyl-CoA desaturase and insulin signaling—what is the molecular switch? *Biochim. Biophys. Acta* **1797**, 1189–1194 (2010).
37. R. J. Heath, Y. T. Yu, M. A. Shapiro, E. Olson, C. O. Rock, Broad spectrum antimicrobial biocides target the FabI component of fatty acid synthesis. *J. Biol. Chem.* **273**, 30316–30320 (1998).
38. J. Boursier, A. M. Diehl, Implication of gut microbiota in nonalcoholic fatty liver disease. *PLoS Pathog.* **11**, e1004559 (2015).
39. M. Mouzaki *et al*., Intestinal microbiota in patients with nonalcoholic fatty liver disease. *Hepatology* **58**, 120–127 (2013).
40. X. Zhang *et al*., Ablation of cytochrome P450 omega-hydroxylase 4A14 gene attenuates hepatic steatosis and fibrosis. *Proc. Natl. Acad. Sci. U.S.A.* **114**, 3181–3185 (2017).
41. E. C. Park *et al*., Inhibition of CYP4A reduces hepatic endoplasmic reticulum stress and features of diabetes in mice. *Gastroenterology* **147**, 860–869 (2014).
42. J. P. Hardwick, D. Osei-Hyiaman, H. Wiland, M. A. Abdelmegeed, B. J. Song, PPAR/RXR regulation of fatty acid metabolism and fatty acid omega-hydroxylase (CYP4) isozymes: Implications for prevention of lipotoxicity in fatty liver disease. *PPAR Res.* **2009**, 952734 (2009).
43. G. Gaich *et al*., The effects of LY2405319, an FGF21 analog, in obese human subjects with type 2 diabetes. *Cell Metab.* **18**, 333–340 (2013).
44. A. Sanyal *et al*., Pegbelfermin (BMS-986036), a PEGylated fibroblast growth factor 21 analogue, in patients with non-alcoholic steatohepatitis: A randomised, double-blind, placebo-controlled, phase 2a trial. *Lancet* **392**, 2705–2717 (2019).
45. J. Seo *et al*., Atf4 regulates obesity, glucose homeostasis, and energy expenditure. *Diabetes* **58**, 2565–2573 (2009).
46. T. Lundåsen *et al*., PPARalpha is a key regulator of hepatic FGF21. *Biochem. Biophys. Res. Commun.* **360**, 437–440 (2007).
47. S. Gesta, Y. H. Tseng, C. R. Kahn, Developmental origin of fat: Tracking obesity to its source. *Cell* **131**, 242–256 (2007).
48. V. Tremaroli, F. Bäckhed, Functional interactions between the gut microbiota and host metabolism. *Nature* **489**, 242–249 (2012).
49. E. F. Murphy *et al*., Composition and energy harvesting capacity of the gut microbiota: Relationship to diet, obesity and time in mouse models. *Gut* **59**, 1635–1642 (2010).
50. A. D. Dayan, Risk assessment of triclosan [Irgasan] in human breast milk. *Food Chem. Toxicol.* **45**, 125–129 (2007).